Light Alternative Vehicle Frame Fatigue Failure Prediction and Prevention

Cameron Daugherty, Gretchen Follstaedt and Mark Archibald

Abstract

Light Alternative Vehicles (LAVs) such as bicycles provide transportation, recreation, competition, and exercise for people around the globe. Due to very limited power, minimizing weight is an important factor in LAV design. Consequently, optimizing frame geometry is also important, and preventing fatigue failure is a significant design task. In the past this was done with expensive and time consuming physical tests but in recent years Finite Element Analysis (FEA) has become the main method for optimizing frame geometry. Peterson and Londry recommended a static vertical gravitational load of three times the acceleration of gravity as a surrogate for a fatigue analysis. This method has proven satisfactory but not optimal as frames were excessively heavy due to overdesign. In 2008, the ASTM International published ASTM F2711, a standard for bicycle frame fatigue that includes both a horizontal and vertical fatigue test. This study investigates the applicability and effectiveness of the vertical test portion of this standard as the basis for an improved early design stage method for design against fatigue failure in LAV frames. A protocol for testing recumbent bicycle frames (which are not explicitly covered by the standard) is also developed and validated. During the course of this study thirteen frames were tested to failure including six upright frames and seven recumbent frames. ASTM F2711 is shown to be a less conservative test for fatigue failure – valuable for early fatigue life design and frame optimization in both recumbents and upright bicycles.

Introduction

Light Alternative Vehicles (LAVs) comprises a class of vehicles dominated by bicycles, but which also includes electric bicycles, velomobiles, and similar vehicles. LAVs are small, and powered either by human muscles or auxiliary power up to 750W[1]. These vehicles provide transportation, recreation, competition, and exercise for people around the globe. As a transportation alternative, LAVs are inexpensive, efficient, and often non-polluting. In urban areas, significant use of LAVs may provide a more sustainable transportation option.

Due to very limited power, minimizing weight is an important factor in LAV design. Consequently, optimizing frame geometry is also important, and preventing fatigue failure is a significant design task. There is a need for fatigue information on light alternative vehicle frames, particularly for custom manufacturers, because fatigue data on frames is not readily accessible to engineers outside of large manufacturing environments. Large, high-quality bicycle manufacturers conduct fatigue research on their frames and do not publish their data[2]. This makes designing different types of vehicle frames for long fatigue life difficult. Peterson and Londry presented a set of finite element analyses in 1986 that included a surrogate fatigue analysis[3]. Today, Finite Element Analysis (FEA) programs are readily available to vehicle designers, and are used to reduce design cycle time and improve product quality. Physical testing takes many times longer than the FEA simulations. Peterson and Londry recommended a static vertical gravitational load of three times the acceleration of gravity as a surrogate for a fatigue analysis. The rational was that if the frame was designed for 3G vertical loading, it would most likely survive actual operational loads that could lead to fatigue failure.

In practice, the 3G vertical load test has proven satisfactory, but not optimal. Peterson and Londry provided little guidance regarding factors of safety, or even what strength is most appropriate. Students designing vehicles at Grove City College have discovered that frames designed such that maximum stress incurred during a 3G vertical load analysis was less than the estimated endurance limit were not prone to fatigue failure, but were excessively heavy due to overdesign. A more accurate method for design against fatigue failure is needed. To be widely useful, such a method would need to be easy to apply in the early design stages and rely only on readily available data (preferably tensile data alone).

In 2008, the ASTM International published ASTM F2711, a standard for bicycle frame fatigue that includes both a horizontal and vertical fatigue test. This study investigates the applicability and effectiveness of this standard as the basis for an improved early design stage method for design against fatigue failure in LAV frames. Two other goals related to application of ASTM F2711 include developing a protocol for testing recumbent bicycle frames (which are not explicitly covered by the standard) and validating the ability to conduct fatigue tests in accordance with ASTM F2711 in the Grove City College laboratory.

Several used bicycle frames were available for initial testing and verification of the apparatus. As such, they were primarily inexpensive commercial frames of unknown load history and material condition. The goals of testing these frames were to 1) verify the capability of testing bicycle frames to ASTM standards, and 2) to verify the accuracy of FEA models and the ability to predict fatigue failure based on FEA analysis. (Note that the ASTM standards do not allow testing on frames with unknown load histories for approval. However, these frames provided an inexpensive and convenient way to meet the study objectives.)

ASTM F2711 was adapted for recumbent frames and six identical frames were built and tested to failure at varying stress levels. Unlike the upright frames, these frames had a known load history and material condition. The goals of testing these frames were to 1) develop methods for applying ASTM standard F2711 to recumbent bicycles, and 2) to apply the ability to predict fatigue failure based on FEA analysis and develop an S/N curve.

Background

Bicycle fatigue testing standards exist to provide information on how to correctly perform a fatigue test that accurately evaluates the fatigue strength of a vehicle frame. ASTM F2711 defines testing methods for bicycle frames. Three tests are defined, a horizontal fatigue test, a vertical fatigue test, and an impact test. Loads applied for each test depend on the frame classification, defined in ASTM F2043. The basis of classification ranges from condition 0 – children's bicycles – to condition 3, which includes downhill grades on rough trails with speeds exceeding 40 km/hr. ASTM standards F2843, F2802, F2868, and F2614 define standard specifications for frame conditions 0 through 3, respectively. The specifications include specific load/cycle combinations for the fatigue tests. Most adult bicycles fall under the condition 2 classification. The horizontal loading fatigue test for condition 2 frames requires a frame to complete a minimum of 100,000 cycles with a cyclic load of 800 N tensile and 600 N compressive applied at the front dropouts along a line which connects the front dropouts to the rear dropouts. The vertical loading fatigue test for condition 2 frames specifies a frame must complete a minimum of 50,000 cycles with a cyclic load of 1200 N to 120 N compression

applied to the seat tube in the vertical direction. These standards are written for upright frames and are not directly applicable to recumbent frames. Figure 1 shows the geometry required for a vertical loading fatigue test[2,5].

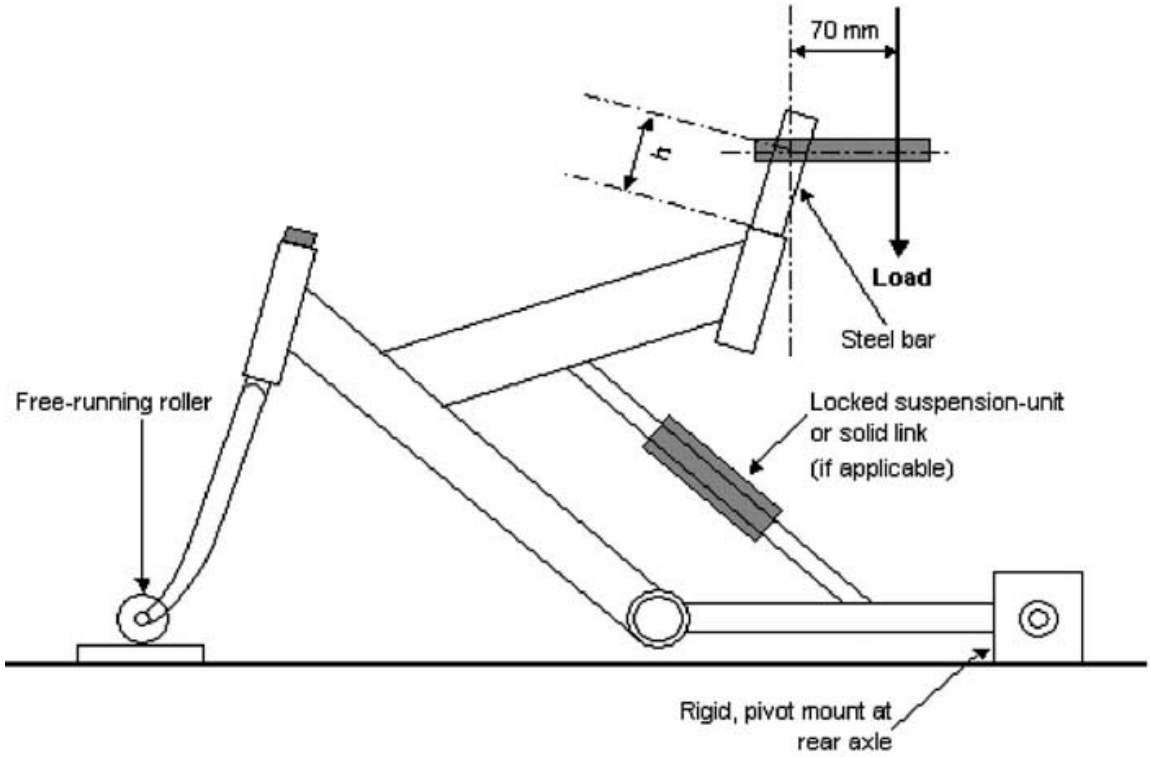

Figure 1 ASTM Standard for Fatigue Testing (Source: ASTM Standard F2711).

Metal fatigue occurs when a material is subjected to repeated loading. Fatigue strength, which depends on material condition, is the stress level which results in failure at N number of cycles. Many materials, including steel, exhibit fatigue or endurance limits, or a stress level below which no number of stress cycles will produce failure[6]. The endurance limit is related to the ultimate tensile strength, being approximately half the tensile strength for a small, polished test specimen tested in pure flexure[7]. Most materials, including aluminum alloys, do not exhibit an endurance limit, implying that a fatigue failure may eventually occur at any stress level. A particularly useful tool for predicting fatigue behavior is the stress-cycles to failure, or S-N diagram. An S-N diagram is a graph of the magnitude of cyclic stress against a logarithmic scale of cycles to failure. Most steel alloys exhibit a knee at around one thousand cycles in which the curve shallows and then becomes flat at around one million cycles[8]. The second knee corresponds to the endurance limit. S-N curves are usually found experimentally and are effected by many factors including material condition and geometry. A useful approximation for an S-N curves for steel can be made by connecting the points (10^3, $0.9S_{ut}$) and (10^6, S_e) on a semi-log scale[7].

Most published fatigue data is based on fully reversed stress cycles. (A fully reversed stress varies between equal positive and negative peak values, and has a mean value of zero.) Frequently, stresses are not fully reversed during cyclic loading. Fluctuating stresses with a mean greater than zero are referred to as tensile mean stresses and those with a mean less than

zero as compressive mean stresses. Typically, tensile mean stresses are more damaging than compressive mean stresses[9]. Figure 2 illustrates the stress components associated with fluctuating stress. Data for this figure was obtained during fatigue testing of a recumbent bike frame in accordance with ASTM F2711. The maximum and minimum stresses are the extreme values, and the stress range is the difference between them. The mean stress is average of the maximum and minimum, and the stress amplitude is one-half of the stress range.

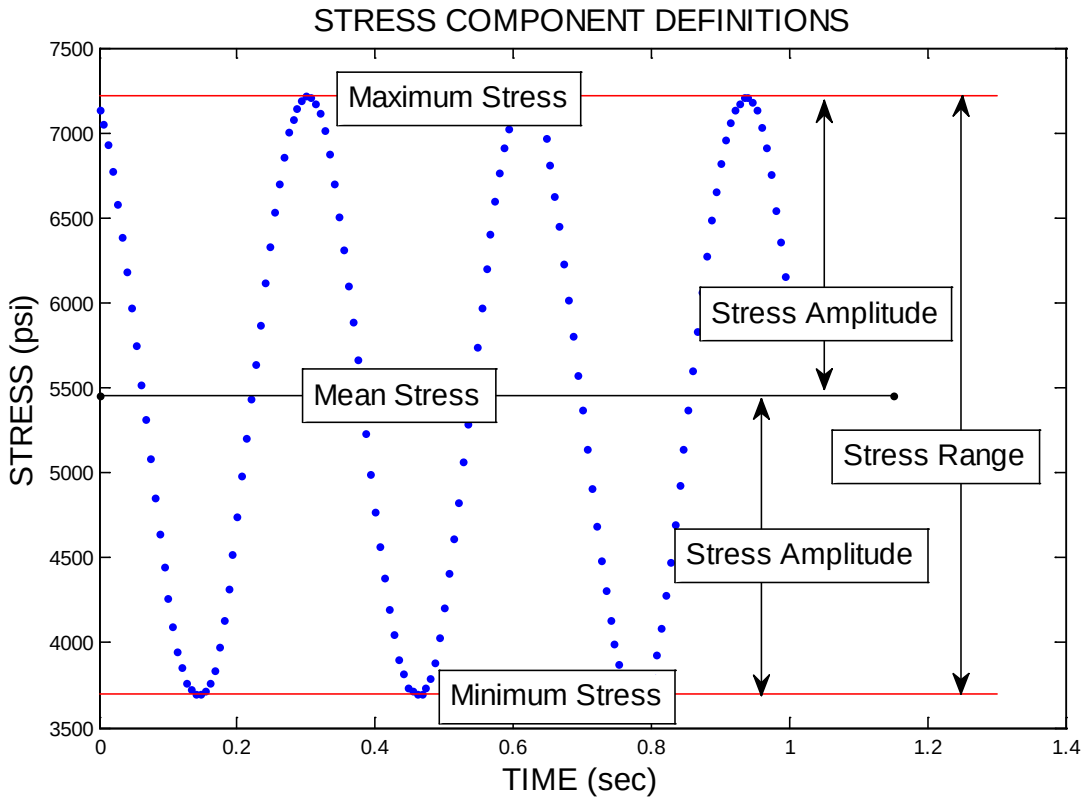

Figure 2 Example of fluctuating stress illustrating definitions of stress components.

Fatigue failure theories have been developed to predict failure under fluctuating stress at a high number of cycles. The Modified Goodman theory is frequently used in design, as it is both simple and conservative[10]. Either the Gerber or the ASME elliptic theories are more accurate for predicting failure than the conservative Modified Goodman theory[7]. When plotted on a diagram of midrange stress versus alternating stress, points above the line indicate predicted failure. The formulas for all three theories are presented in Equation (0.1) and plotted in Figure 3.

Modified Goodman: $\frac{\sigma_a}{S_e}+\frac{\sigma_m}{S_{ut}}=1$

Gerber: $\frac{\sigma_a}{S_e}+\left(\frac{\sigma_m}{S_{ut}}\right)^2=1$ (0.1)

ASME Elliptic: $\left(\frac{\sigma_a}{S_e}\right)^2+\left(\frac{\sigma_m}{S_{ut}}\right)^2=1$

σ_a = alternating stress
σ_m = midrange stress
S_e = endurance strength
S_{ut} = ultimate strength

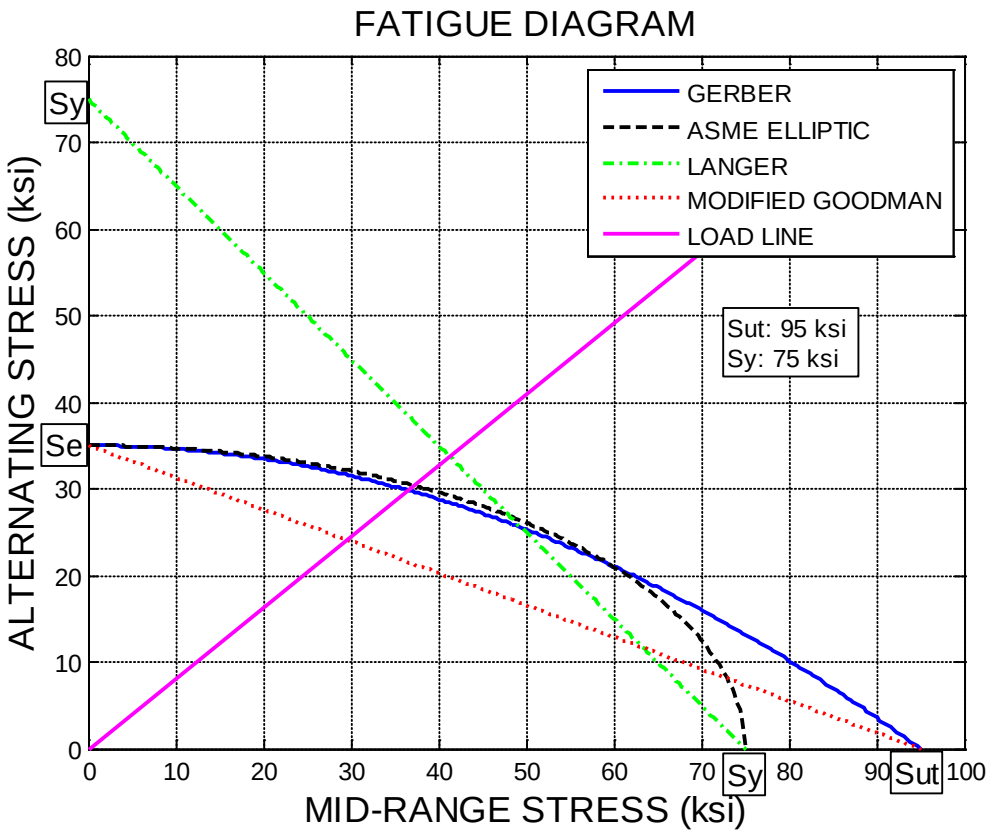

Figure 3 Plot of the mean stress equations and a load line consistent with ASTM F2711 (minimum stress is one-tenth of the peak stress).

The mean stress equations presented in Equation (0.1) can be modified as shown in Equation (0.2) to relate any mean and alternating stress combination to an equivalent fully reversed stress that is expected to cause the same amount of damage[10]. These equivalent fully reversed stresses can then be used with published S-N diagrams to make life cycle predictions.

$$D = \sum \frac{n_i}{N_i}$$

$$\sigma_{rev,Goodman} = \frac{\sigma_a}{1 - \frac{\sigma_m}{S_{ut}}} \qquad (0.2)$$

$$\sigma_{rev,Gerber} = \frac{\sigma_a}{1 - \left(\frac{\sigma_m}{S_{ut}}\right)^2}$$

D = accumulated damage

n_i = number of cycles at a stress level σ_{rev}

N_i = number of cycles to failure at σ_{rev}

σ_{rev} = equivalent fully reversed stress

Finite element analysis is used in structural engineering to model and predict many quantities, including mechanical stresses, through the subdivision of a mathematical model into a finite number of elements, connected by nodes. When a load is applied to the structure, the elements, which can be thought of as springs, deform due to loads transmitted by the interconnected nodes.

Finite element programs determine the deformation of the elements and the corresponding displacements of the nodes. Stresses can then be computed for each element based on Hooke's law, which relates stress to strain. FEA programs usually provide graphical output for a variety of measures, such as stress, deflection, and strain energy[11]. The accuracy of an FEA model depends strongly on the manner in which the structure is modeled, constrained, and loaded. One must clearly define the loads to be applied to the structure, including location, direction, type, and magnitude. Once the load case is defined the challenge becomes interpreting the results and identifying acceptable stress values. In the past Peterson and Londry recommended a static vertical gravitational load of three times the acceleration of gravity as a surrogate for a fatigue analysis (see Figure 8). This method has proven satisfactory but not optimal as frames were excessively heavy due to overdesign. Applying ASTM F2711 allows a new load case to be developed with a smaller but more concentrated 270 lb. load applied vertically downward at a 70 mm offset to the seat tube.

Methods

A testing apparatus (fatigue tester) capable of vertical fatigue tests on either upright or recumbent bicycle frame was designed and constructed during the 2012/2013 academic year. The fatigue tester was developed by a team of senior mechanical engineering students at Grove City College in fulfillment of their capstone design requirement (see Figure 4 below). The fatigue tester used the frame of a Satec T5000 tensile testing machine. All electronic and control systems were replaced with Aerotech controls and an Aerotech servo motor. An Omega strain gage amplifier and signal conditioner module provided for strain inputs, and the existing 5000 lb. load cell used on the Satec frame was retained. The load cell was professionally re-calibrated according to ASTM Standard E74 and the amplifier gains were set accordingly. Cross-head position was provided by the Aerotech servo motor controller, programmed to account for the belt drive reduction ratio and the lead of the ball screws. Controls were programed using LabVIEW in conjunction with an Aerotech BM 1400 brushless motor, an Aerotech Soloist controller, and Aerotech subroutines. Load application during the tests was force controlled, i.e. a load point was maintained, not a stress or strain level. Each test was programmed to run for a certain number of cycles, or until failure was detected.

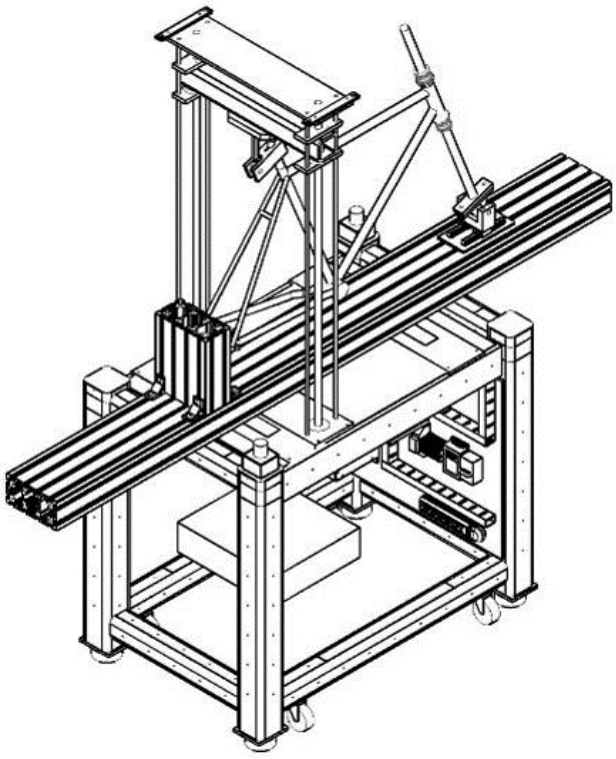

Figure 4 Fatigue testing machine.

Before testing, each of the frames were carefully measured to determine tube diameters and lengths. Where possible, wall thickness was measured. Where non-destructive measurement of wall thickness was not possible, reasonable guesses were initially made. Wall thickness was measured after testing by cutting the tubes out of the frame. Hardness tests were also conducted on the frames at several locations to estimate the tensile strengths. These estimated values were compared with published data for low carbon cold-rolled butt-welded (CRBW) tubes, which appeared to be the material used for most of the frames. The endurance limit was estimated to be half the ultimate tensile strength times the Marin modification factors for surface condition and size (tube diameter), as shown in Equation (0.3) below. A contour plot like the one shown in Figure 5 can be a particularly useful when applying these equations. It is a rather crude way of estimating fatigue properties, but is consistent with the desire to develop an early design stage method for predicting fatigue failure with minimal data.

$$
\begin{aligned}
S_e &= k_a k_b S'_e \\
k_a &= 2.70 S_{ut}^{-0.265} \\
k_b &= 0.879 d^{-0.107} \\
S'_e &= 0.5 S_{ut}
\end{aligned}
\qquad (0.3)
$$

k_a = surface condition modification factor
k_b = size modification factor
S'_e = rotary-beam test specimen endurance limit
S_e = endurance limit at critical location in condition and geometry of use

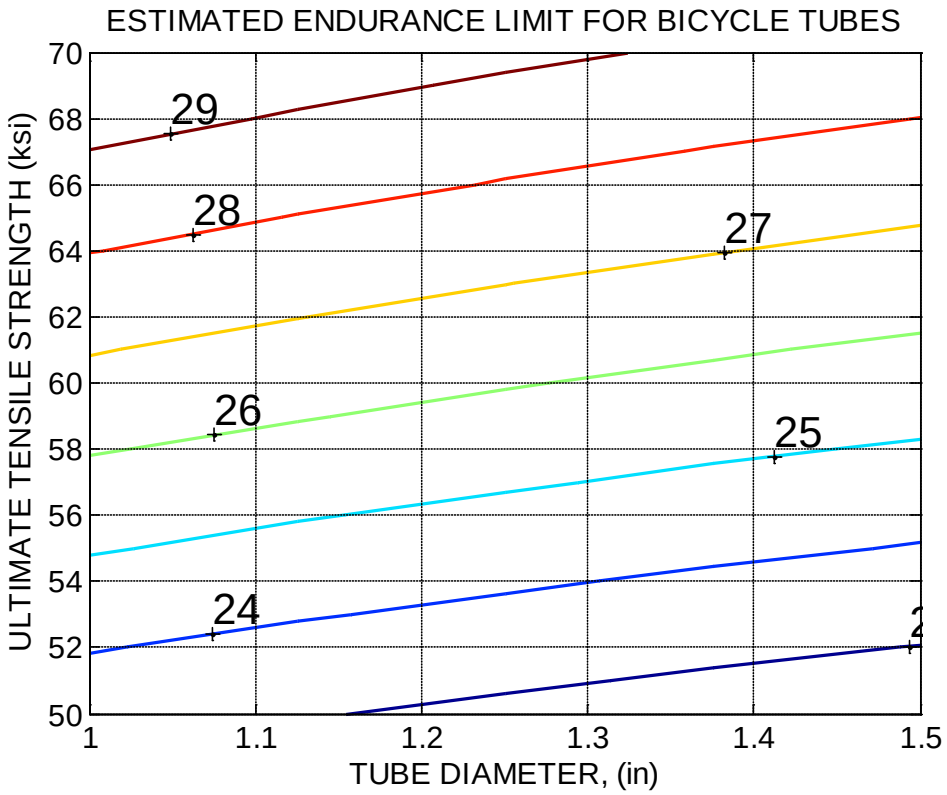

Figure 5 Plot of the estimated endurance limit as a function of the tube diameter and ultimate tensile strength based on the Marin modification factors presented in Equation (0.3).

A beam idealization like the one in Figure 6 below is probably the quickest and easiest way to get rough estimates for stresses in a frame. This method is adequate for use early in the design stage but lacks the geometry to provide stress concentrations at critical joints, and were insufficient to estimate fatigue failures. Shell idealizations are a more accurate model of stress concentrations. No geometry is lost in the model, so stresses from corners, joints, and holes are better accounted for. The beam model would not have led to a prediction of failure at the end of the seat post, which was the point of failure for the upright frames.

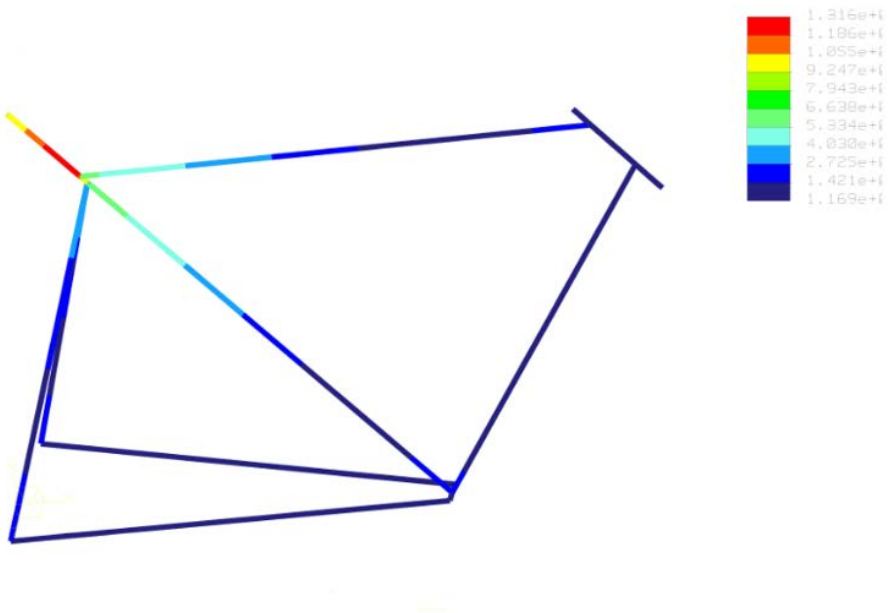

Figure 6 Beam idealization for upright frame.

FEA shell models and load cases for each frame were developed to simulate both the ASTM vertical load fatigue test and the 3G vertical drop test (see Figure 7, 8, respectively). Care was exercised in developing the frame model and establishing interfaces between components. There are large changes in geometry around joints which can cause difficulties during analysis. In order to prevent this, surface regions were created on the shell about 1/8" from the joint. It would be impossible to model every feature of every frame, so decisions were required regarding appropriate level of detail – sufficient for analytical purposes without undue modeling burden. Weld fillets were not included in the FEA model because the welds on the frames are not of a consistent radius. A solid, rigid seat post was used to apply the load. Each strain gage was accounted for by a point measure representing the center of the strain gage. These point measures were later compared with strain gage values to ensure they correlated well.

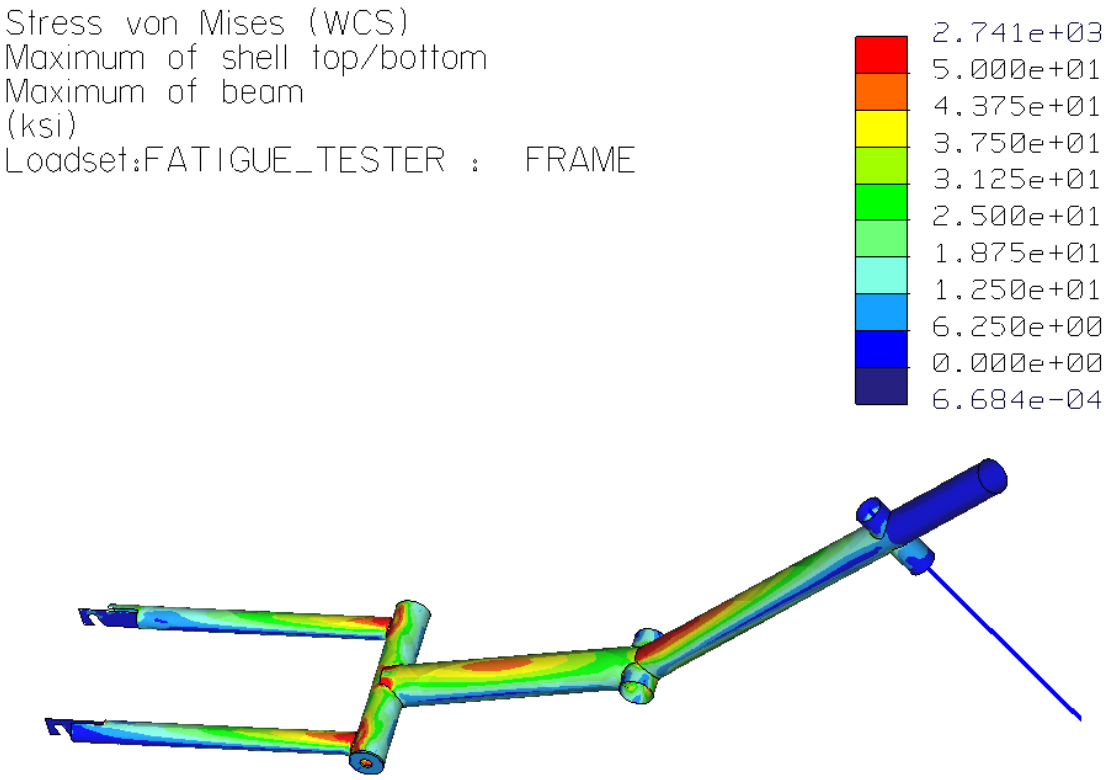

Figure 7 FEA Shell model with adapted ASTM F2711 270 lb. load.

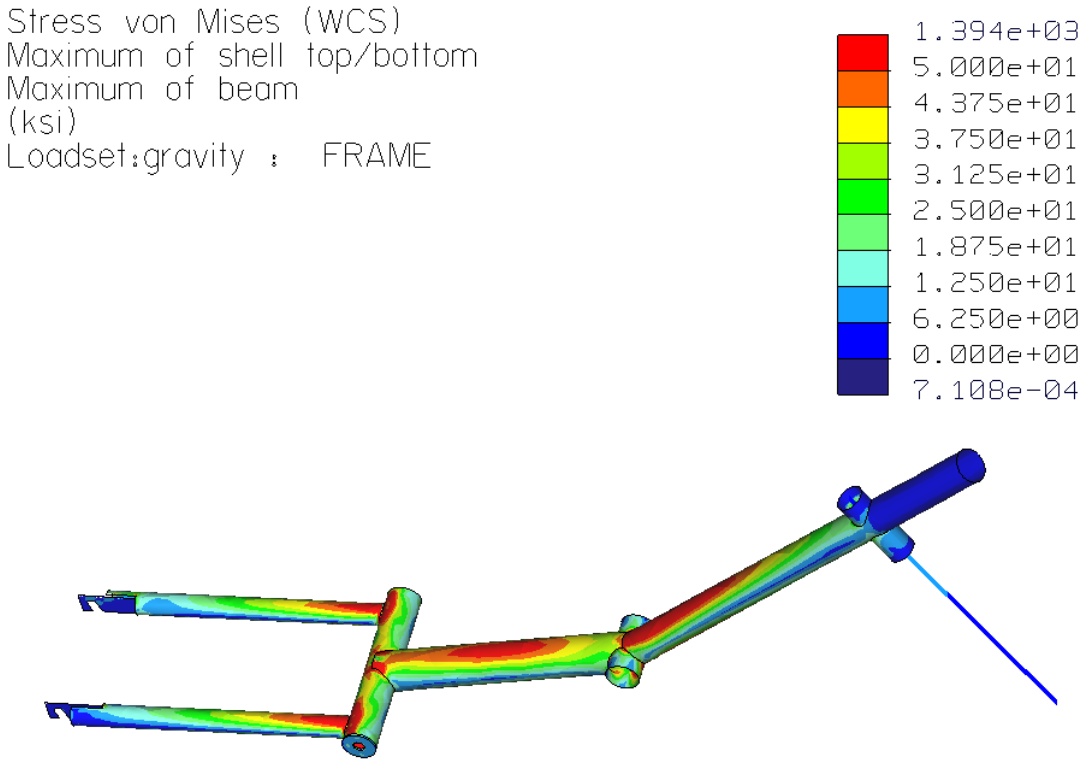

Figure 8 FEA Shell model with 3G vertical load. Note that the stresses are higher than in the ASTM F2711 load case.

Strain gage locations were chosen based on preliminary FEA models to provide optimal data for comparing the FEA model and strain gage data. A single strain gage was always placed away from steep stress gradients, in which the strain can vary significantly over the length of the gage. However, it was placed near areas of high predicted stress. On several of the upright frames strain gages were placed directly on top of what we predicted to be the highest stress concentration at the end of the dummy seat post. This gave a view of the strain behavior right at the failure point even though plastic damage was sustained, precluding the use of stress-life theories.

A procedure was developed to calibrate strain gages using calibration resistors on the Omega strain amplifier boards. Initially, strain gage channel calibration was verified using an independent Instron tensile test machine and double checked against an existing strain gage data acquisition system with known calibration. Subsequently, each strain gage was applied and shunt calibrated prior to the frame being tightened down in the fixture. After the frames were fitted with strain gages they were fixtured in the fatigue tester. Care was taken to minimize unintentional stresses from fixturing the frame by putting spacers on the rear axle so that the chain stays did not flex when tightened down. On upright frames the dummy seat tube was carefully inserted to a known depth to ensure the FEA model was accurate. After the frame was fixtured, the strain readings were checked at zero load to ensure there were no offsets.

Six identical recumbent frames were constructed for testing. The frames were of welded steel construction, made from MIL-T-6736B seamless aircraft tubes. The welds were made using the tungsten-inert gas (GTAW) process with ER80D2 filler rod. For each recumbent two strain gages were used: one linear gage and one rosette. The linear gage was placed on the down-tube of the frame, one inch from the end of the tube and parallel to the tube's axis. The rosette gage was placed on the bottom of the transverse tube, 5/8" from the center of the weld of along the axis of the chain stay. See Figure 9 for strain gage locations and frame geometry.

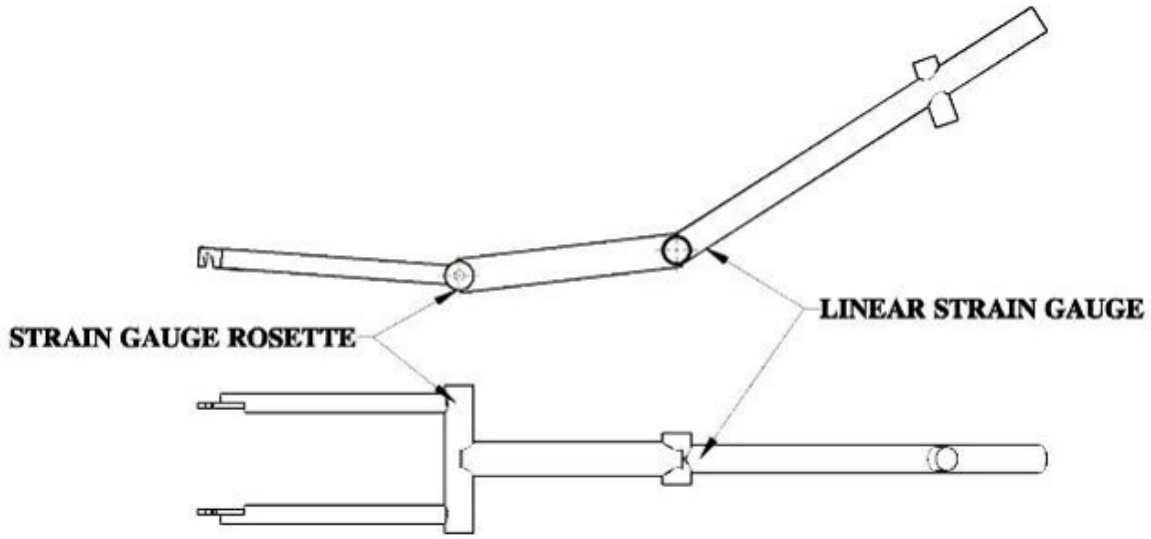

Figure 9 Strain gage locations on recumbent frames.

ASTM F2771 is not specifically applicable to recumbent bicycle frames because the load is

applied to the seat tube, a component many recumbent frames lack. A protocol for testing recumbent frames is needed. Since a recumbent frame does not use a seat post, and consistency with the existing standard is desired, the load was applied directly to the frame at a location under the seat. If the seat is adjustable, the load should be positioned such that the flexural moment is maximized. This protocol was used on all frames that did not meet ASTMs definition of an upright frame.

To plan tests on the upright frames, hardness values were used to estimate tensile strength and from that the endurance limit. The recumbent frames, made from 4130 chromoly steel tubing, had a minimum ultimate tensile strength of 95 ksi. With the Marin modification factors given in Equation (0.3) the endurance limit of the 1" chainstays was estimated to be approximately 37 ksi. These parameters were used to plot the Gerber, ASME elliptic, and Langer yield line mean stress equations along with the load line using stress values from the FEA model (Figure 3). In all cases the load fluctuated between the peak value and a minimum value one-tenth of the peak. This was based on maintaining the same stress ratio as prescribed in the ASTM standard. The intersection of the load line with any of the failure theories is the failure prediction point. The failure prediction point was then used to set the load level on the fatigue tester. This allows either load or strain to be set to the desired level for a test to failure at the estimated endurance limit. If the stress level is increased further, the modified mean stress equations given in Equation (0.2) can be used to calculate an equivalent fully reversed stress to plot on an S-N curve, and from that predict the number of cycles to failure. If an S-N curve is unavailable, this methodology can be used to plan a series of tests to derive one. Each test can be run a different stress level to generate a series of points which can then be connected with linear regression to form an S-N curve.

Results

In all but one of the upright frames failure occurred at the end of the dummy seat post, on the tensile stress side. At the end of the seat post a horizontal crack formed and propagated around the circumference of the tube. There were no other signs of damage on the upright frames. All failures in the recumbent frames occurred through the weld at the bottom of the transverse tube connecting to the chainstays. The cracks in almost all cases initiated at the edge of the weld in the heat affected zone but propagated through the center of the welds along the notched edge of the chainstay.

Figure 10 Typical recumbent frame fatigue failure along the chainstay weld.

All of the frames tested passed the vertical fatigue test described in ASTM F2711, even though they were designed and manufactured before the standard was first published. Almost all sustained hundreds of thousands of additional cycles at much higher loads before failure. Two of the bikes didn't fail until loads well in excess of 1000 lbs were applied. Table 1 shows the most severe loading sustained by each frame and the number of cycles to failure at that load level. Note that all upright frames were tested at 1200 N (270 lbs) for 100,000 cycles, or twice the ASTM requirement, prior to testing to failure. The recumbent frame tested at 270 lbs made it past the required 50,000 cycles but eventually failed at 247,000. Passing ASTM standards does not mean the bicycle will not eventually fail, as 50,000 cycles is well within the finite life region for steel, which is about 1,000,000 or 10^6 cycles.

Table 1 Summary of fatigue tests for upright and recumbent frames. Strain values for upright frames are from linear gage placed at the seat-tube concentration point. Strain values for the recumbent frames are from the linear down-tube gage.

Bike ID	**Bike Type**	**Number of Cycles**	**Load** (lbs)	**Peak Strain** (microstrain)	**Min. Strain** (microstrain)	**ASTM Vertical Load Test**
2	Upright	54,520	630	1266	28	Passed
4	Upright	445,690	600	1726	140	Passed
6	Upright	11,520	1050	2393	652	Passed
7	Upright	83,900	1340	N/A	N/A	Passed
11	Recumbent	13,692	487	2655	283	N/A
12	Recumbent	33,904	490	2525	219	N/A
13	Recumbent	36,553	480	2450	190	N/A
14	Recumbent	57,513	430	2281	240	N/A
15	Recumbent	246,877	270	1378	186	Passed
16	Recumbent	1,290,000	175	911	137	N/A

Tests of the recumbent frames provided valuable data for constructing a load-life curve for this frame. It is expected that the peak vertical force corresponding to the endurance limit is at or near 780 N (175 lbs), although additional tests would be needed to verify this. The load-cycles to failure behavior can be fit by an exponential function, given by Equation (0.4) and shown in Figure 11 below.

$$S_F = 6272N^{-.251} \qquad (0.4)$$

This load-life relationship (which is not the traditional stress-cycles to failure relationship) can be used to predict failure in frames of similar geometry. In the future, when students are designed frames and performing FEA analysis, they will be able to make comparisons to the ASTM F2711 load case shown in Figure 7 with knowledge of the load-life performance shown in Figure 11. As noted above, Equation (0.4) is not a traditional S-N relationship. The choice to present a load-life relationship was made because the rosette gage readings were difficult to reconcile with the FEA model.

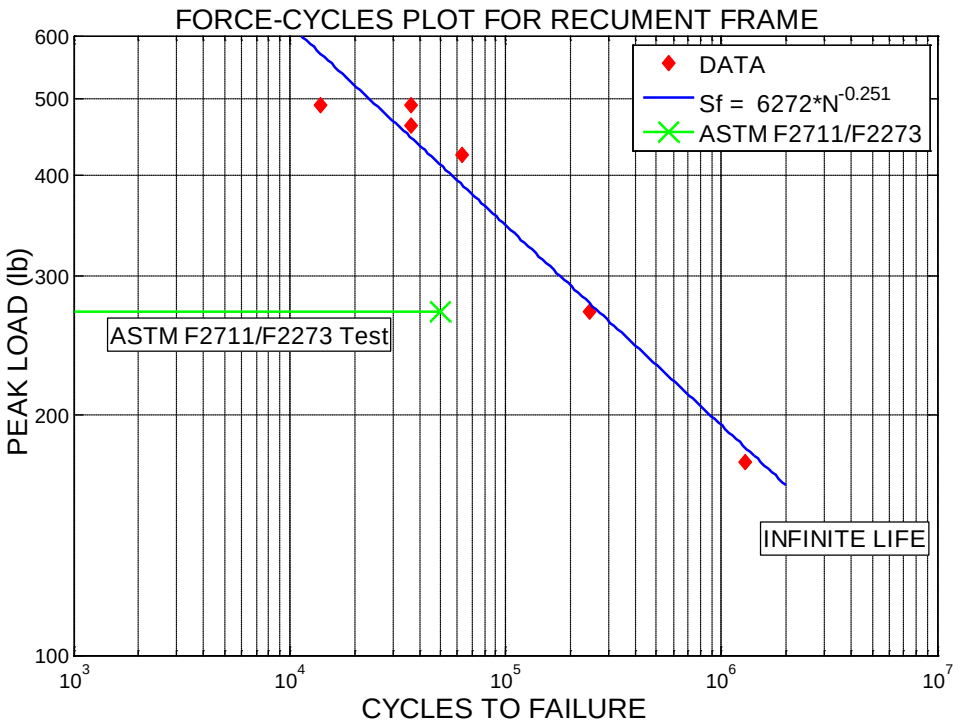

Figure 11 Load-Life plot for recumbent bicycle frames. Note the load-cycles line representing ASTM F2711 falls within the finite life region but well to the left of the failure line.

The choice to use a strain gauge rosette instead of multiple linear gages was made out of a desire to understand the full stress state at a critical and complex location, and to compare the experimental values to the analytical FEA models. The strain gage rosettes were difficult to reconcile with the FEA model and discrepancies precluded their use in further analysis.

The initial tests run on six upright bicycle frames verified the ability to conduct fatigue tests in accordance with ASTM F2711. These tests also verified the accuracy of the FEA models. Comparison of the FEA analysis with the collected data has shown the FEA values are within 10 to 20% of the actual values for locations sufficiently far away from stress concentration points. The method developed for testing recumbent frames by applying a bearing load to the worst case position for the seat proved adequate. The recumbent frame intentionally designed to be marginal passed the test and survived for another 200,000 cycles.

Conclusion

This study verified that the Grove City College testing apparatus can successfully conduct fatigue tests in accordance with ASTM standards for vertical fatigue tests on steel bicycle frames. Further, it has validated the ability to predict if a frame design will pass or exceed the ASTM standards. FEA can be used for analysis, provided care is used in modeling. Beam element idealizations are not sufficient for predicting fatigue failures. However, they may still be used early in the design stages to rapidly converge to an acceptable gross geometry – if suitable factors of safety are used. FEA models using shell idealizations can realistically predict actual stresses during a fatigue test. FEA modeling has shown that the ASTM fatigue test results

in models which are less conservative. Physical tests on these bikes confirmed the FEA stress levels, and the ability of the frames to sustain the loading. Additional work is being done to predict the behavior of welds in thin-walled steel structures and estimate joint strength under fluctuating stresses, particularly with respect to weld size and filler material.

References

1. Archibald, Mark, “Analysis Of Light Alternative-Powered Vehicle Use And Potential In The United States”, Proceedings of the ASME 2011 International Mechanical Engineering Congress & Exposition, November 11-17, 2011, Denver, Colorado, USA.
2. Lindsey, Joe. "Bikes and Gear Features." Specialized Bikes Test Lab. N.p., n.d. Web. 2 Aug. 2013.
3. Peterson, Leisha A., and Kelly J. Londry. "Finite-Element Structural Analysis: A New Tool for Bicycle Frame Design." Bike Tech Summer 1986. Print.
4. ASTM International, ASTM F2711-08, Standard Test Methods for Bicycle Frames, 2008.
5. ASTM International, ASTM F2868-10, Standard Specification for Condition 2 Bicycle Frames, 2010.
6. Bhat, S., and R. Patibandla. “Metal Fatigue and Basic Theoretical Models: A Review.” (2011): 1-35.
7. Budynas, Richard G., J. Keith. Nisbett, and Joseph Edward. Shigley. Shigley's Mechanical Engineering Design. New York: McGraw-Hill, 2011. Print.
8. Pook, L. P. “Metal Fatigue: What It Is, Why It Matters.” Dordrecht: Springer, 2007. Print.
9. Boardman, Bruce. "Fatigue Resistance of Steels." ASM Handbook, Volume 1: Properties and Selection: Irons, Steels, and High-Performance Alloys (1990): 673-88.
10. Dowling, N. "Mean Stress Effects in Stress-Life and Strain-Life Fatigue." SAE Technical Paper 2004-01-2227.
11. Archibald, M. “Design of Human Powered Vehicles.” *Forthcoming*.